THE JOURNAL OF PHYSICAL CHEMISTRY B

ARTICLE

pubs.acs.org/JPCB

Millisecond Time-Scale Protein Dynamics Exists Prior to the Activation of the Bulk Solvent Matrix

Gusztáv Schay,[†] Levente Herényi,[†] Miklós Kellermayer,[†] Károly Módos,[†] Takashi Yonetani,[§] and Judit Fidy*[,†,‡]

[†]Semmelweis University Budapest, Department of Biophysics and Radiation Biology, P.O. Box 263, H-1444 Budapest, Hungary

[‡]Research Group for Membrane Biology, Hungarian Academy of Sciences, Budapest, Hungary

[§]Department of Biochemistry and Biophysics, University of Pennsylvania School of Medicine and the Johnson Research Foundation, Philadelphia, Pennsylvania 19104-6059, United States

Supporting Information

ABSTRACT: Conformational dynamics of proteins is of fundamental importance in their physiological functions. The exact mechanisms and determinants of protein motions, including the regulatory interplay between protein and solvent motions, are not yet fully understood. In the present work, the thermal activation of phosphorescence quenching was measured in oxygen-saturated aqueous protein solutions to explore protein dynamics in the millisecond range. The sample was brought to cryogenic temperatures in a fast cooling process to avoid the bulk crystallization of ice. The phosphorescence quenching effect was followed by the phosphorescence lifetime of either Zn-protoporphyrin substituting the heme in the β-subunits of human hemoglobin (Zn-HbA) or tryptophan residues of Zn-HbA and human myoglobin (Mb), measured in thermal equilibrium at temperatures varied from 8 to 273 K. The quenching effect was attributed primarily to the activation of collisions with O_2 molecules made possible by the activated millisecond time-scale dynamics of the matrix around the chromophores. We find that, in the studied temperature range, the activation of protein global dynamics facilitating oxygen diffusion takes place at clearly separated lower temperatures and independently from bulk solvent dynamics and that the energy and entropy differences between the studied frozen and thermally activated states are specific for the protein.

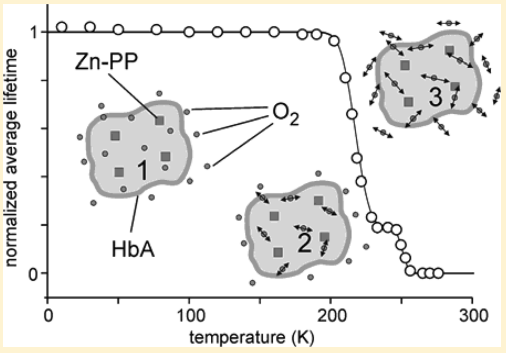

INTRODUCTION

The conformational dynamics of proteins is known to be an extremely complex phenomenon.[1,2] It is a hierarchical network of specific motions across several orders of magnitude of spatial and temporal scales. Some dynamic components are observable even at cryogenic temperatures,[3] whereas others become activated around the "glass transition temperature" of proteins. The time scale may extend from picoseconds to the time range of seconds.[4−9] It is therefore experimentally demanding to monitor a wider scale of these motions in a single research approach[10,11] since the various experimental and computational methods refer to specific time windows of motions. Most of the results have been obtained on myoglobin, which has thus become "the H-atom of biophysics"[12] due to its advantageous properties as a model system.[13] The time window of the applied methods in most cases was in the submillisecond range.[14] Some motions involved in biologically relevant reactions (e.g., domain motions, closure of loops), however, take place in the millisecond−second range. It is therefore of functional significance to develop and utilize techniques that address this longer time scale of protein dynamics.[2,15−17]

Although the functional significance of conformational dynamics is becoming more and more accepted,[1] our understanding of dynamics regulation and of exact mechanisms of action in macromolecular interactions is far from complete.[18] Especially intriguing questions are related to the role of the protein environment in its internal fluctuations. These important questions may involve coupling to the dynamics of the hydration layer, the bulk buffer, the crowded environment of the cell, or motions in any specific interface bordering the molecule.[19−25] The answer must be found for each time and amplitude scale of the involved motions. It has been suggested, for example, that a strong coupling occurs between the internal protein dynamics and fast fluctuations in the hydration shell, whereas slower motions on a larger scale are slaved to fluctuations in the bulk solvent.[26] The experimental techniques applied in the studies often involve optical measurements at cryogenic temperatures on samples containing high percentages of glycerol. It is relevant to

Received: July 20, 2010
Revised: January 19, 2011

dx.doi.org/10.1021/jp106755t | J. Phys. Chem. B XXXX, XXX, 000–000

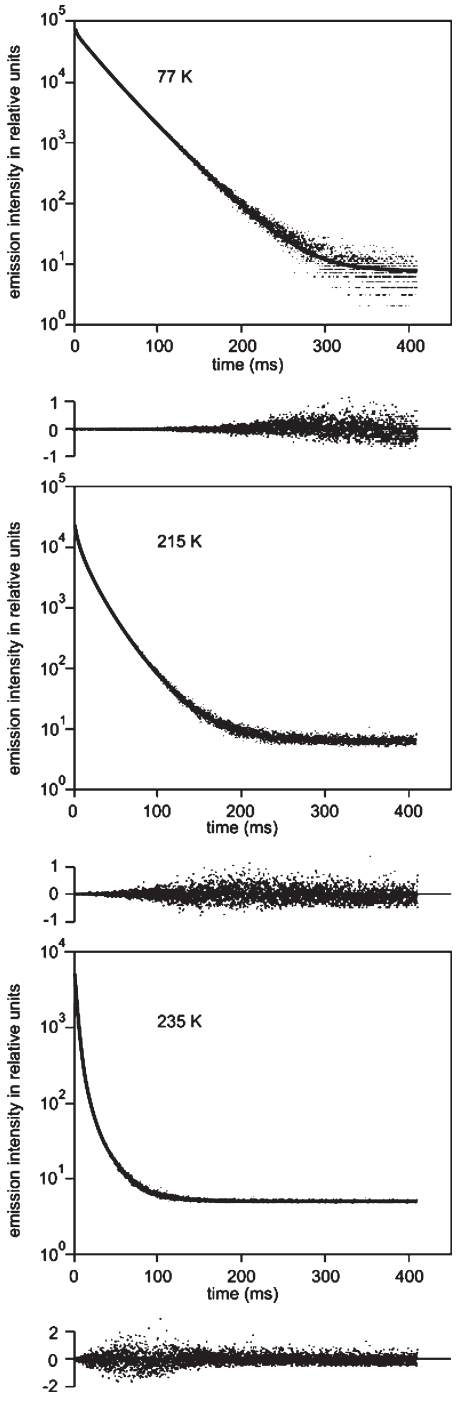

Figure 1. Triplet-state decay data of Zn-HbA and functions (continuous line) fitted with a sum of 4−5 exponentials at three different temperatures (77, 215, and 235 K), in semilogarithmic representation. The relative error of data points and the fitted curve is also presented.

investigate how this circumstance may influence the conclusions concerning the dynamic coupling of protein and its environment.

In this paper, we report results on the thermal activation of large-scale protein dynamics in the time window of 30−600 ms in aqueous buffer, in the absence of cryosolvents. We report that millisecond-range protein dynamics coupled to the hydration layer can be activated well below the temperature at which bulk solvent dynamics becomes activated. We show that the activation temperature and related thermodynamic parameters are specific for the protein and that in the presence of glycerol the activation of protein motions cannot be separated from the dynamics of the bulk glassy solvent.

MATERIALS AND METHODS

Sample Preparation. Sodium chloride, dimethyl sulfoxide (DMSO), and 4-(2-hydroxyethyl)-1-piperazineethanesulfonic acid (HEPES) were purchased from Aldrich-Sigma (St. Louis). All samples were prepared in 100 mM HEPES, pH 7.4, with deionized water, containing 100 mM NaCl. Hybrid human hemoglobin (HbA) with zinc protoporphyrin-IX (Zn-PP) substituting the heme in the β subunits, $[\alpha\text{-}FeO_2]_2\text{-}[\beta\text{-}Zn]_2$-HbA (Zn-HbA), was prepared in T. Yonetani's Laboratory at the University of Pennsylvania.[27] Cl^- ions were added to the samples in the form of NaCl (100 mM). Human myoglobin (Mb) from Aldrich-Sigma (St. Louis) was used as purchased. The protein concentration was 60 μM in all experiments.

Adjusting the Temperature of the Sample. We report phosphorescence lifetime data obtained on samples in thermal equilibrium, at varying temperatures starting from 8 K. The adjustment of the initial low temperature of the sample and of the higher temperatures was done by using a Cryophysics M22 type closed-cycle helium refrigerator (Cryophysics SA, Geneva, Switzerland) and LakeShore M330 temperature controller (LakeShore, Inc., Westerville, USA). Using the cryostat, its coldfinger of copper must be brought into and kept in good thermal contact also under vacuum conditions. The sample of 80 μL volume was contained in a quartz (UV fused silica) tube of 2.7 mm inner diameter, sealed gastight with a conical Teflon stopper. The techniques required for the present study had to achieve the following conditions: (1) to bring the sample to 8 K fast enough to avoid phase separation and bulk crystallization of the aqueous sample, (2) to maintain the thermal contact of sample and coldfinger in a broad temperature range from 8 to 273 K, (3) reproducibility of the structural conditions in the sample.

1. Cooling to 8 K. Fast cooling was achieved by using a copper adapter attached to the coldfinger prepared with an indium-coated hole that contained the sample tube with a tight fit. Prior to the insertion of the sample, the copper housing was precooled to 77 K by liquid nitrogen. The positioning of the sample in the cryostat was fast, and the low temperature of the housing promoted fast cooling. The data obtained by this method, however, showed that the good thermal contact between the sample tube and coldfinger could not be maintained at higher temperatures (>200 K).

2. Maintaining the Thermal Contact of the Sample Tube and Coldfinger in a Broad Temperature Range. Another copper adapter fixing the contact of the sample tube and the coldfinger by springs achieved good thermal contact in the full temperature range of the experiments. In this method, however, the positioning of the sample in the cryostat required more time than to put it in a hole, thus precooling to 77 K made no sense. The coldfinger in this method was first precooled to 240 K by the cryostat. At this temperature, the tube was fixed, and the cryostat was closed, evacuated, and continued cooling to 8 K by the highest cooling rate. Phosphorescence lifetime data were determined at various increasing temperatures starting from 8 K on samples cooled either by the "fast cooling" method (with precooling to 77 K) or by the second method (with precooling to 240 K) for comparison. The data showed identical temperature dependence in the

dx.doi.org/10.1021/jp106755t |J. Phys. Chem. B XXXX, XXX, 000–000

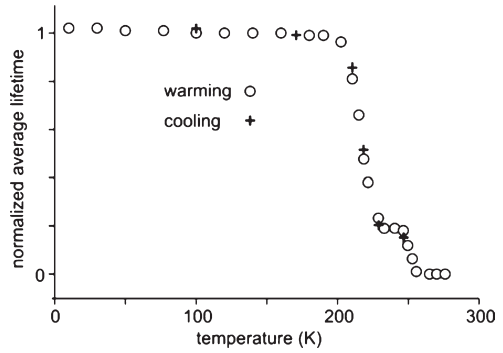

Figure 2. Normalized average phosphorescence lifetime data of Zn-HbA as a function of temperature measured in a stepwise warming process (open circles) and cooling process reverted from 245 K (crosses).

two cases (see Figure S1 in the Supporting Information) if the temperature stayed below 250 K. On the basis of the results of this control study, we selected the second method for cooling protocol in the reported experiments and considered it a "fast cooling" technique. We found that the results obtained by this protocol were reliable within the whole temperature range of the studies.

3. Reproducibility—Reversibility. In the experiments, we detected phosphorescence lifetime data under thermally activated quenching conditions. The quenched emission signal at higher temperatures was very week, and thus long data collection times were needed. A total measurement time covering the whole temperature range spanned over several days up to a week. Still, parallel experiments involving larger steps on the temperature scale were performed and proved the reproducibility of the data. Reproducibility was lost, however, at lower cooling rates (compare Figures S1 and S2 in the Supporting Information). Slower cooling led to precipitation and deterioration of the protein samples as expected. Besides reproducibility, we found also complete reversibility of the temperature effect on the phosphorescence lifetime if the temperature did not exceed 250 K (see later Figure 2). This experience showed that the selected time period of thermal equilibration at each temperature (45 min) was sufficient in our temperature dependence protocol (see details below).

Oxygen Content of the Samples. In most experiments, the protein solutions were saturated with the oxygen of air by carefully and slowly bubbling air into the samples for 5 min prior to the experiment. Partially oxygen-saturated Zn-HbA samples were prepared using a special procedure. As a first step, the temperature of the sample in air-saturated form was suddenly decreased to 250 K. At this temperature, the pressure was reduced to 10^{-2} mbar, and this low pressure was maintained for 0.5 h. Subsequently, the sample was sealed and further cooled to 8 K. The measurements were then carried out starting from this state like those performed with oxygen-saturated samples. The goal was to achieve partial oxygen saturation without inducing structural changes in the protein. Possible denaturation or change in the redox state of the heme during experiments was controlled by recording the absorption spectrum. No significant changes were detected in the 270−700 nm wavelength range after the thermal cycles or after partial deoxygenation.

Phosphorescence Decay Measurements at Various Temperatures. The phosphorescence lifetime of the samples was determined along with a stepwise warming period starting from cryogenic temperatures. The samples were equilibrated for 4 h at 8 K before starting the heating cycle to ensure thermodynamic equilibrium. Then gradual heating took place in 10 or 5 K increments, and the samples were equilibrated at each temperature selected for data collection for 45 min before the start of one decay measurement. At each temperature the triplet state lifetimes of the chromophores, namely, Zn-PP, palladium coproporphyrin (Pd-CP), or tryptophans (Trp) of the proteins were measured using the time-domain mode of an EAI CD900 spectrometer (Edinburgh Analytical Instruments, Edinburgh, U.K.) equipped with a μF900 Xe flashlamp of a power of approximately 1 mJ/pulse and a pulse width of 2 μs fwhm. Excitation and emission wavelengths for Zn-PP, Pd-CP, or Trp were 409, 384, or 290 nm and 723, 668, or 421 nm, respectively, with 5 nm bandpass. The phosphorescence emission signal was very weak due to light scattering and quenching effects. To reach an acceptable signal/noise ratio for evaluation, up to 14 000 consecutive flashes were summed with a time resolution of 80 μs. The long data collection time involved the possibility of photobleaching. This was controlled by repeated data collection periods and lifetime evaluation. Phosphorescence photons were detected by a photomultiplier tube (R928, Hamamatsu Photonics, Shimokanzo, Japan) operated in single photon counting mode and cooled to 255 K (C65972 cooler). After amplification, data were collected by a Norland 5000 multichannel analyzer card (Viking Instruments, Madison, U.S.A).

Evaluation of Phosphorescence Decay Curves. In the experiments, the goal was to characterize the dynamic state of the selected protein at various temperatures by the phosphorescence lifetime of a specific embedded chromophore. This parameter of chromophores in an ensemble of protein molecules and at an ensemble of dynamic conditions is considered heterogeneous since both the heterogeneous conformational environment and the heterogeneity of the quenching conditions affect the individual lifetimes. We decided to determine the average lifetime of the heterogeneous lifetime population and use it as a dynamic parameter. Two approaches have been applied to determine reliable average lifetimes. We analyzed the decay curves by the method of maximum entropy (MEM), yielding lifetime distributions (data are shown in the Supporting Information) and fitted the decay data ($I(t)$ functions) with the sum of exponential decay functions of discrete lifetime values (eq 1).

$$I(t) = \sum_{i=1}^{n} A_i e^{-t/\tau_i} \quad (1)$$

A_i and τ_i are the amplitudes and lifetimes of the individual components, respectively, and n is the number of exponentials used for the fitting. According to our experience, an acceptable least-squares fit required 4−5 discrete exponentials (see Results and Discussion). The ensemble average $<\tau>$ was taken into consideration according to eq 2.

$$<\tau> = \frac{\sum_{i=1}^{n} A_i \tau_i^2}{\sum_{i=1}^{n} A_i \tau_i} \quad (2)$$

The $<\tau>$ values had a relative error less than 5%.

dx.doi.org/10.1021/jp106755t |*J. Phys. Chem. B* XXXX, XXX, 000–000

Table 1. Parameters of Fitting the Phosphorescence Decay of Zn-HbA Measured at Three Different Temperatures with the Sum of Exponentials of Discrete Lifetimes and the Corresponding Average Lifetimes (<τ>)

		instrument response	strongly quenched	medium quenched	long lifetime components		average
77 K	lifetime (ms)	← 0.9 →		5.7	23.6	35.0	28.4
	rel. amplitude	← 8746 →		5604	41042	22805	
215 K	lifetime (ms)	0.196	2.0	6.3	15.9	31.3	16.0
	rel. amplitude	14941	18741	39639	35777	6206	
235 K	lifetime (ms)	0.6	2.2	4.0	10.1	25.6	6.4
	rel. amplitude	17502	61590	37911	7068	1379	

RESULTS

Phosphorescence Lifetime of Zn-PP in HbA as a Function of Temperature. The intrinsic phosphorescence lifetime of Trp has been suggested for and successfully applied to monitoring the internal dynamics of proteins at room temperature.[28] Since molecular oxygen is a very effective collisional quencher of phosphorescence,[29] these studies have been performed in the absence of oxygen. In our study, instead of deoxygenation, we saturated the samples with air (oxygen) and registered the phosphorescence lifetime in thermal equilibrium at various temperatures starting from 10 K up to 273 K to detect the activation of quenching effects. The chromophores were Zn-PP, substituting the heme in the β subunits of Zn-HbA and the tryptophans of the protein. In low-temperature optical studies, transparency is usually maintained by the addition of cryosolvent. We wanted to refrain from changing the physical parameters of the sample (protein and solvent) and therefore avoided this method. Figure 1 shows examples of phosphorescence decay data of Zn-PP in Zn-HbA on a semilogarithmic plot at various temperatures, the decay curves arising from discrete fittings (eq 1) and the error of the fittings. Although the signal was low due to significant light scattering, with sufficient data collection time, acceptable signal/noise levels could be reached even at higher temperatures, where quenching effects became activated. The discrete lifetime components, the corresponding amplitudes, and the <τ> values (eq 2) are shown in Table 1. The phosphorescence decay data were also evaluated by MEM. The two approaches yielded results with remarkably good agreement, and the ensemble average lifetime values calculated by eq 2 in both cases agreed within experimental error and followed the same trend in function of temperature. (see the comparison of the results of MEM analysis and fittings with discrete lifetime components for the same decay data sets in Figure S3 of the Supporting Information). Lifetime components of the 100 μs range appeared in both methods of evaluation. On the basis of the analysis of the instrument response function and on the fact that the phosphorescence decay was recorded with 80 μs resolution, these were considered as experimental artifacts and were omitted from data evaluation. The next shortest component in both approaches was in the lifetime range of 0.9−2 ms. This component—of low population at lower temperatures—seemed unaffected by the temperature and remained the sole component close to 273 K. We attributed this signal to such chromophores which have trapped oxygen molecules in their immediate vicinity of specific configurations. It is evident from both evaluations that the studied thermally activated quenching affects the value of the lifetime components/distribution function of longer lifetimes (see Table 1 and Figure S3 of the Supporting Information). These longer components evidently will dominate the <τ> values

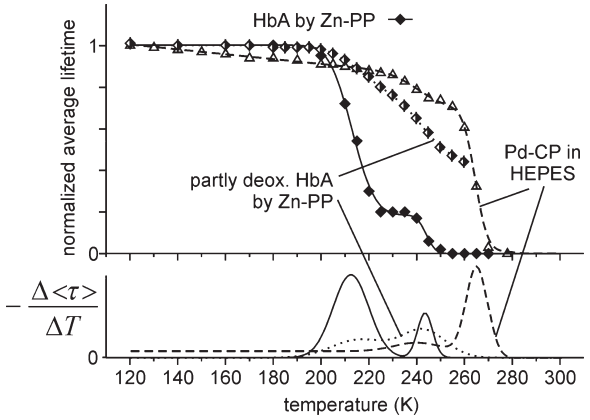

Figure 3. Normalized average phosphorescence lifetime data as a function of temperature (upper part of the figure). The continuous curve corresponds to a thermodynamic model fitted with the data points. The negative derivative function of the fitted curves is also presented (lower part of the figure). Data points and fitted curves are shown for Pd-CP in HEPES buffer (open triangles and dashed line), partially deoxygenated Zn-HbA (half-filled diamonds and dotted line), and oxygen saturated Zn-HbA (filled diamonds and continuous line).

based on either evaluation method. In the further analysis of the average lifetime values in function of temperature, we decided to use the values based on the discrete fitting method, since it uses all 4096 data of the decay function. In the MEM analysis the software uses a reduced number of data (128 in our case) selected from a logarithmic scale. Otherwise, the calculations in MEM would be very demanding computationally. The thermal activation of protein dynamics was thus characterized by $<\tau>_{discr}$, plotted on a normalized scale in function of temperature.

Figure 2 shows the normalized average lifetime of Zn-PP in Zn-HbA as a function of temperature. The lifetime does not change significantly from 10 K up to about 180 K. Above this temperature, quenching effects become activated, and the lifetime drops in two markedly separated steps on the temperature scale. The first step begins at around 190 K and becomes complete at around 230−235 K. The second step follows the first one and completely eliminates the signal. Importantly, the phenomenon is fully reversible along a cooling path if reverted below 250 K—an example is shown in the figure.

Mechanisms Underlying the Two Steps of Phosphorescence Quenching of Zn-HbA. To examine the contribution of the protein matrix to dynamic activation, the phosphorescence lifetime measurement was also performed on a chromophore sample deprived of the protein. Because the solubility of Zn-PP is extremely poor in aqueous buffer, we measured the emission of

dx.doi.org/10.1021/jp106755t |J. Phys. Chem. B XXXX, XXX, 000–000

Table 2. Average Lifetime (<τ>) Data ± s.d. at 10 K Determined by Fitting with Discrete Lifetime Components

sample	<τ> 10 K (ms)
Zn-PP in HbA	28.9 ± 0.8
Trp in HbA	212 ± 22
Trp in Mb	605 ± 44
Pd-CP in HEPES	2.14 ± 0.11
Zn-PP in DMSO, at 100 K	0.11 ± 0.05
Zn-PP in HbA stripped	28.7 ± 0.6

Pd-coproporphyrin (Pd-CP) instead under buffer conditions identical with those of the protein samples. On the basis of literature data from NMR studies on the thermal activation of the mobility of protons coordinated to buffer components in aqueous solutions, referring to the same temperature range as in our study (discussed below), we supposed that the structural coupling of the Zn- or Pd-porphyrin derivatives to the solvent matrix cannot be significantly different. Data starting from 120 K are shown in Figure 3. For comparison, the data for Zn-HbA of Figure 2 are also included. The data were fitted with two sigmoidal functions based on a simple thermodynamic model (see Discussion). To better characterize the two steps in the quenching effect, the negative derivative functions of the fitted curves are also presented in the figure. In the case of Pd-CP, in the low-temperature range, a gradual and slight quenching effect appears to be activated. Then, well above the temperature range of the first quenching step in Zn-HbA, a slight step is detected at around 240 K. At approximately 265 K, near the melting point of ice, complete quenching occurs. The slight quenching step at around 240 K is comparable with results of proton NMR relaxation experiments in the 500 μs time range and is attributed to the activation of hydrogen motions in structured water regions around the components of aqueous buffers.[30,31] Thus, we identify this step with the mobilization of structured water around the porphyrin molecules and the buffer components. The quenching experiment was also performed on Zn-PP dissolved in DMSO. This solvent was selected because it has no phase transition in the studied temperature range. Although the intrinsic lifetime was strongly quenched by the sulfur of DMSO (Table 2), the signal was measurable up to 274 K. A gradual quenching effect without any steps was observed (see Supporting Information Figure S3) corresponding to a matrix without phase transition in the studied range.

To sum up, without the protein matrix, the low-temperature step observed in the quenching experiment with Zn-HbA is absent. From NMR studies, the temperature range is available for the activation of proton motions in the hydration layer of proteins. The similarity of this range and that of the first step in the phosphorescence quenching effect suggests that the hydration layer and the protein are dynamically coupled and supports our conclusion that the low-temperature step in the quenching experiment on Zn-HbA should be attributed to the activation of motions in the protein matrix around the chromophore.

Role of Collisions with O_2 Molecules in the Quenching Effect. The role of collisions with O_2 molecules in the quenching effect was studied by comparing the data obtained on the fully air-saturated sample with those of the partially deoxygenated sample in the case of Zn-HbA (see Figure 3). The comparison indicates that partial depletion almost completely eliminates the low-temperature quenching step, while the second step remains

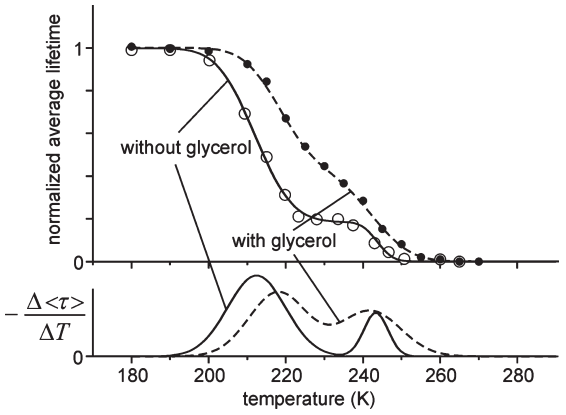

Figure 4. Normalized average lifetime data of Zn-PP phosphorescence in HbA as a function of temperature and the negative derivative functions of the fitted curves in HEPES buffer (open circles and continuous line) and with 60% (v/v) glycerol (filled circles and dashed line).

barely detectable. In this sample, total quenching occurs only around the thawing temperature of ice. These observations showed not only that the low-temperature step detected in oxygen-saturated protein samples is related to activated motions in the protein but also that these motions are permissive of oxygen diffusion. In both the protein and the aqueous matrix, the diffusion of oxygen requires the activation of large-scale motions.[4] The results indicate that the activation temperature of such motions of the protein (possibly forming a unified dynamic unit with its hydration layer) and of the matrix are clearly distinguishable, and that of the protein is lower.

Activation of Millisecond Motions in the Protein and in the Solvent May Not Be Separated in the Presence of Glycerol. It has been suggested that large-scale motions, e.g., those allowing hopping of small molecules in the conformation or allowing the uptake or release of such ligands, are "slaved" to α fluctuations in the solvent environment through long-range dipole−dipole interactions, while their internal local vibrations follow the behavior of β fluctuations of their hydration shell.[32] The experimental techniques underlying these models often involved optical spectroscopy at low temperature using the standard method of adding cryosolvent (glycerol) in quite high percentages (up to even 90%) to the aqueous buffer of the protein solution to avoid light scattering, to extend the measurable range of kinetic parameters, and to avoid the possible structural effects of crystalline ice formation during cooling.

To test the effect of cryosolvents, the phosphorescence quenching experiment was repeated on Zn-HbA in the presence of 60% (v/v) glycerol (see Figure 4). Glycerol changes both quenching steps, shifting their characteristic temperature ranges closer to each other. The increase in the temperature of the first step (from 213 to 220 K) we attribute to the effect of increased viscosity on protein dynamics.[33] The lowered temperature of the second step (to 240 K) is comparable to the phase transition point of concentrated glycerol/water mixtures (−34.7 °C ≈ 238 K for 60% (w/w) glycerol content). The two-step feature of the quenching effect becomes observable only in the derivative representation, whereas in the lifetime vs temperature function, the two steps fuse into a single step, easily attributable to the activation of motions in the solvent, which is of glassy nature in the case of high glycerol content. In such a case the slaving of large-scale protein dynamics to α fluctuations of the solvent

dx.doi.org/10.1021/jp106755t |J. Phys. Chem. B XXXX, XXX, 000–000

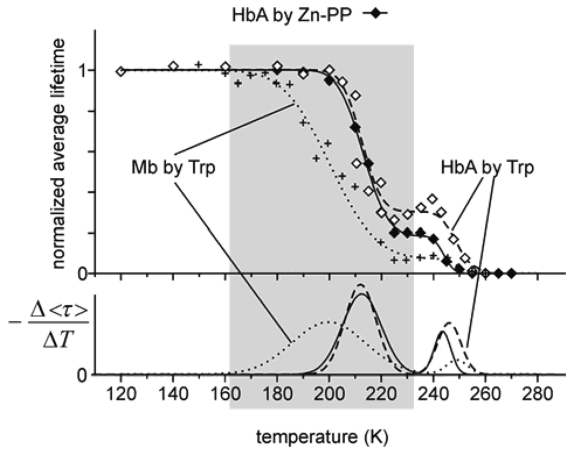

Figure 5. Normalized average lifetimes and negative derivative functions of the fitted curves of Zn-PP and Trp in HbA (filled and open diamonds and continuous and dashed lines, respectively) and Trp in native Mb (crosses and dotted line), in the 120−280 K temperature range. The range of protein-related transitions is marked with a gray shaded area.

above T_g (now ~210 K)[34] may be a good approximation since the T_g value of the protein and that of the glassy solvent almost overlap with each other. The relation of protein dynamics and solvent dynamics remains hidden under these conditions. We underline another important outcome of the glycerol effect: the shift of the activation temperature of protein dynamics directly proves that it is sensitive to the structure and the dynamic nature of its immediate environment.

The ability of high glycerol concentrations (>65%) to cause even protein denaturation is another point which should not be overlooked.

Same Protein Dynamics Is Observed Either by Porphyrin or by Tryptophan Phosphorescence. To prove that the observed dynamics monitored by Zn-PP in the β subunits is not the property of the heme environment, but is characteristic of the whole protein, we carried out dynamics activation experiments based on the Trp phosphorescence of Zn-HbA. The protein contains six Trp residues. The Trp lifetimes were relatively short[24] even at low temperatures (Table 1) due to self-quenching and energy transfer to the hemes[35] but could be determined with acceptable precision. The Trp lifetime data compared with the data of Zn-PP are shown in Figure 5. The first quenching step marked with gray shading is very similar in the two kinds of monitoring, indicating that the effect reflects the global behavior of the Zn-HbA matrix. The slight difference in the second step, observable in the derivative representation, may be an artifact originating from the increased error of Trp-based data or caused by differences in the oxygen diffusion pathways from the external solvent matrix to the site of the different chromophores (heme or Trp).

First Quenching Step Is Specific for the Protein. The use of Trp phosphorescence allowed us to compare the phosphorescence quenching effect in two different proteins. We selected human Mb having two Trp's for comparison dissolved in the same buffer as HbA (see Figure 5). The first phase of lifetime decrease is significantly different in the two distinct proteins, whereas the second quenching step becomes activated at nearly identical temperatures for both proteins. Thus, the first step in the thermal activation of quenching is characteristic and specific for the global millisecond dynamics of the protein under study.

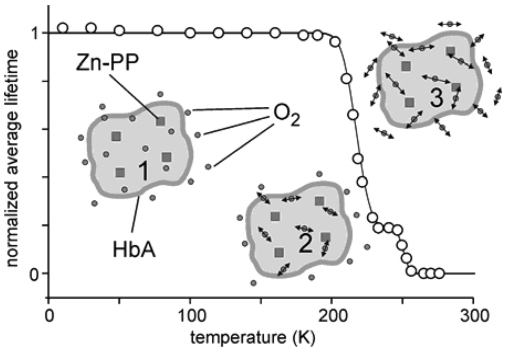

Figure 6. Normalized average lifetime data of Zn-PP phosphorescence in HbA at different temperatures as in Figure 2 with the fitted curve. Cartoons refer to states 1 (frozen ms dynamics up to about 200 K), 2 (plateau after dynamic activation of protein and coupled boundary), and 3 (state after the second step with activated dynamics also in the solvent).

DISCUSSION

Qualitative Model of the Thermal Activation of Millisecond Protein Dynamics. Proton NMR studies in the ~500 μs time window of motions in bovine serum albumin (BSA) in a temperature range similar to the one investigated in our study yielded data for the proportion of mobilized water protons in the hydration layer around the protein, in water regions coordinated to the buffer components, and in icy structures of the buffer, selectively.[30,31] The cooling and warming protocol in these studies was very similar to our method. No mobile water molecules were observed below 220 K, and the mobilization of the hydration layer around BSA became activated above this temperature, detected as an abrupt increase in the number of mobile protons. When the temperature was further increased, mobilization of the structured water around the buffer components was first observed as a separate phenomenon on the temperature scale, and then upon warming further, the melting of the bulk icy matrix followed. These data provide strong support for the idea that the activation of large-scale protein dynamics seen in our experiments is coupled to the activation of dynamics in its surrounding hydration layer. Our conclusion concerning the thermal activation of the millisecond range of motions in our protein samples is outlined in Figure 6. "State 1" in this model is the frozen state, in which oxygen is equally immobile in the bulk solvent, in the hydration layer of the protein, and inside the protein matrix. We hypothesize that during the first, low-temperature step of phosphorescence quenching motions within the protein and in its closely coupled boundary become activated. This leads to a dynamic state of limited oxygen diffusion in the coupled system ("State 2"). When the temperature is further elevated, oxygen diffusion becomes activated also in the matrix, causing a final reduction of the phosphorescence lifetime below the detection limit of our instrumentation ("State 3").

Thermodynamic Parameters of Protein Dynamics Activation. We suggest a simple thermodynamic model to interpret the experimental data concerning protein dynamics activation. The model thus refers to the first step of the process (transition from "State 1" to "State 2" in Figure 5). On the basis of the previous considerations, by the term "protein" from now on, we understand the protein molecule in dynamic coupling to its bordering hydration layer. The model ignores the details of molecular

dx.doi.org/10.1021/jp106755t |J. Phys. Chem. B XXXX, XXX, 000–000

mechanisms and assumes that "State 2" corresponds to activated collective dynamics in the protein and in its closely coupled boundary. This coupled system is considered as a single particle in the sample from a thermodynamic point of view. At a certain temperature, the individual particles fluctuate between energy states, and the probability to find a single particle in its mth microstate with E_m energy is P_m. We suppose that P_m is proportional to the respective Boltzmann factor as

$$P_m \sim e^{-E_m/kT} \tag{3}$$

We suppose that the particles are identical and independent, and in the frozen state of the environment (during the first transition) they are distinguishable. Thus, on the basis of ergodicity, the distribution of energy ($P(E)$) is given as

$$P(E) \sim \Omega(E) \cdot e^{-E/kT} = e^{-(E - TS)/kT} \tag{4}$$

where $\Omega(E)$ is the number of microstates which have E energy. Since the entropy is given as $S = k \ln \Omega$, where k is the Boltzmann constant, one may further develop the equation into the final form of eq 4. In equilibrium states this formula can give the respective equilibrium values of the physical quantities. In the model we suppose two energy states: "1", frozen with a long average lifetime, τ_0 (= intrinsic lifetime), and "2" (higher energy state), with activated quenching that leads to an average lifetime τ_d, decreased by a factor of K_d: $\tau_d = \tau_0/K_d$.

If the number of molecules in the two states "1" and "2" are N_0 and N_d, respectively, the average lifetime of the ensemble can be calculated in this model as

$$<\tau> = \frac{\sum_{i=1}^{n} N_i \tau_i}{\sum_{i=1}^{n} N_i} = \frac{N_0\tau_0 + N_d\tau_d}{N_0 + N_d} = n_0\tau_0 + n_d\tau_d \tag{5}$$

where n_0 and n_d are the relative number of particles without and with activated dynamics, respectively. For the comparison of data obtained on different chromophores and proteins, it was useful to normalize the average lifetime data

$$\frac{<\tau>}{\tau_0} = n_0 + n_d\frac{\tau_d}{\tau_0} = n_0 + \frac{n_d}{K_d} \tag{6}$$

Since every measurement was carried out in thermal equilibrium, we may use eq 4 to determine the expected value of the relative number of particles (n) in a given state. Thus, it follows

$$\frac{n_d}{n_0} = e^{-(\Delta E - T\Delta S)/RT} \tag{7}$$

Here ΔE and ΔS are the (molar) energy and entropy differences between the frozen and thermally activated states of the particle. Taking into account that the number of particles is constant ($n_0 + n_d = 1$), and substituting the expressions for n_0 and n_d into eq 6, we obtain eq 8 that yields the temperature dependence of the relative average lifetime, which can be directly fitted to the average lifetime data obtained from the measurements (eq 2).

$$\left(\frac{<\tau>}{\tau_0}\right)(T) = \frac{\left(1 + \frac{1}{K_d}e^{-(\Delta E - T\Delta S)/RT}\right)}{(1 + e^{-(\Delta E - T\Delta S)/RT})} \tag{8}$$

The parameters of the fitted curves derived from the derivative representation (transition midpoint temperature (T_{MP}) and maximum slope value (Sl_{MP})) are obtained as

$$T_{MP} = \frac{\Delta E}{\Delta S} \text{ and } Sl_{MP} = \frac{\Delta S}{4RT_{MP}}\left(\frac{1}{K_d} - 1\right) \tag{9}$$

In the figures, the solid lines fitted to the data points correspond to eq 8 in the case of the first step. The model clearly fits the experimental data very well, and the fitting thus yielded the thermodynamic parameters of the function. For the second step, we used a sigmoid curve for fitting since we could not interpret this range by a molecular model. The thermodynamic parameters concerning the first step are shown in Table 3.

Table 3. Parameters of Fitting the Thermodynamic Model to the First Step of Activated Quenching: ΔE (Energy Change), ΔS (Entropy Change), T_{MP} (Midpoint Temperature), and K_d (= τ_0/τ_d), ± s.d.

sample	ΔE (kJ/mol)	ΔS (J/mol·K)	T_{MP} (K)	K_d
HbA (Zn-PP)	97.7 ± 5.6	456 ± 29	214.2 ± 0.7	5.3 ± 0.3
HbA (Trp)	93.0 ± 13.8	435 ± 76	213.9 ± 5.6	4.0 ± 0.7
Mb (Trp)	36.2 ± 6.0	182 ± 37	198.7 ± 4.9	10.6 ± 1.7
HbA stripped	113.4 ± 4.4	532 ± 22	213.1 ± 0.3	2.0 ± 0.1

Analysis of the Thermodynamic Parameters. The magnitude of the energy difference in Table 3 is comparable to the energy of a few hydrogen bonds. The entropy change is comparable to the denaturation entropy of about 2−5 amino acid residues.[36] These literature data encourage us to build up a view of the thermally activated quenching mechanism as collisions with O_2 molecules involving an average "hop distance" (mean free path) of a length of a few (2−5) residues. Thus, collisional quenching is made possible by a limited, anisotropic diffusion process inside the protein and in its coupled surroundings (similarly to ligand diffusion in Mb (see, e.g., refs 37−39)), by "hopping" through transiently opening spaces, which are created by the global dynamics of the structure. Our simple thermodynamic model fits the experimental data and yields realistic parameters.

Since the normalized average lifetime data for quenching activation in Zn-HbA were very similar in the case of Zn-PP- or Trp-monitoring, the thermodynamic parameters are also very similar. One may ask whether one has to consider the possible effect of the relatively high Cl^- concentration on protein dynamics since Cl^- is generally considered as an allosteric effector of oxygen binding to the heme in HbA, binding primarily to the central cavity of the quaternary structure of HbA.[40] We compared the quenching effect found in the presence of NaCl and in a stripped condition of HbA (see Supporting Information Figure S4). Slight, but significant, differences were found in the presence of Cl^-. It was experimentally found that the dimer dissociation constant of Zn-HbA is bigger in the presence of chloride ions.[32] Putting this observation together with our present data, the loosening of subunit (dimer) contacts in this case correlates with an increased probability of activated global (dimer) dynamics in Zn-HbA. (We note that this conclusion refers to the T (deoxy)-like HbA structures since Zn hybrid hemoglobin structures were classified as part of the T-like family[41].)

There is a significant difference in the thermal activation of quenching between HbA and Mb (Figure 4), also manifested in the thermodynamic parameters. Apparently, the conditions in Mb significantly increase the probability of activated quenching

dx.doi.org/10.1021/jp106755t |J. Phys. Chem. B XXXX, XXX, 000–000

based both on the energy and entropy difference values. In addition, the significantly lower activation temperature (T_{MP}) in Mb implies that in this case the energy difference is relatively less significant than the entropy difference between the activated and nonactivated states (eq 9). The increased K_d points to a greater efficiency of quenching in Mb.

It is difficult to establish a detailed molecular basis that explains the difference in the activation of millisecond dynamics between Mb and HbA. The thermodynamic model that yields the compared parameters describes both cases as ensembles of independently fluctuating molecules. Thus, monomeric Mb molecules are compared to tetrameric Hb. A first look at the enormous number of data concerning the cooperative behavior of HbA subunits in oxygen binding would suggest that they should evidently form a dynamically coupled unit. A closer look, however, yields very little direct information on the details of this dynamics coupling, e.g., on how the presence of the interfaces would influence the overall dynamics, whether there is a size effect involved, etc. Reported results of molecular dynamics simulation are based on techniques that address different questions.[42] Dissociation studies suggest that the separation of the tetramer into dimers requires less energy than dissociation into monomers,[43] thus this contact seems to be looser, which may also affect the strength of dimer−dimer dynamic coupling. Although studies by the Ackers group on the cooperative behavior of HbA formed of asymmetrically mutated dimers lead to the conclusion that the dimers behave "autonomously" in the cooperative oxygen binding effect,[20] one would expect more evidence for declaring the dimers to be dynamically uncoupled units in HbA. If this were the case, however, then the dynamic difference between Mb and HbA could be related to the very interesting dynamic role of the hydration layer in the case of Mb versus that of the subunit interface partially bordering HbA dimers. The results concerning the dynamic effect of the presence of Cl^- should also be in line with dynamic constraints exerted by the dimer interface. In lack of sufficient evidence, at present, the molecular reason for the dynamic difference between Mb and Hb remains unresolved.

CONCLUSIONS

It was shown that millisecond time-scale broad range dynamics in protein molecules coupled to their bordering coordinated layers can be activated at lower temperatures and thus independently from the activation of dynamics in the aqueous bulk solvent. The solvent influences the internal dynamics only through the dynamic properties of the bordering layer at the protein surface. Therefore, protein dynamics in the studied time and amplitude range is not solely the consequence of solvent dynamics but is an independently existing phenomenon. This dynamic property of protein solutions may become hindered in the presence of high concentrations of glycerol. The increased viscosity shifts the activation temperature of intrinsic protein dynamics to higher temperatures, and the activation temperature of motions in the glassy bulk solvent will be different from that in an aqueous buffer. Therefore, the use of cryosolvents in protein dynamics studies requires careful considerations from this aspect.

ASSOCIATED CONTENT

Supporting Information. In this document, we present data concerning the validity of the cooling procedure applied in the experiments being a "fast" cooling technique; we present results of the evaluation of phosphorescence decay curves by the method of maximum entropy; and we present detailed data of the studied thermally activated phosphorescence quenching reactions in the case of two systems used as reference in our work: Zn-HbA under stripped condition and ZnPP dissolved in DMSO. This material is available free of charge via the Internet at http://pubs.acs.org.

AUTHOR INFORMATION

Corresponding Author

*Fax: +36 1 2666656. E-mail: judit.fidy@eok.sote.hu.

ACKNOWLEDGMENT

J. Fidy and G. Schay acknowledge support from the Hungarian Academy of Sciences through the Research Group for Membrane Biology. G. Schay is thankful for travel grants of the American Biophysical Society to attend the annual meetings. The authors acknowledge helpful discussions with L. Smeller and A.D. Kaposi.

REFERENCES

(1) Henzler-Wildman, K. A.; Lei, M.; Thai, V.; Kerns, S. J.; Karplus, M.; Kern, D. *Nature* **2007**, *450*, 913–916.
(2) Henzler-Wildman, K. A.; Kern, D. *Nature* **2007**, *450*, 964–972.
(3) Zollfrank, J.; Friedrich, J.; Vanderkooi, J. M.; Fidy, J. *Biophys. J.* **1991**, *59*, 305–312.
(4) Frauenfelder, H.; Sligar, S. G.; Wolynes, P. G. *Science* **1991**, *254*, 1598–1603.
(5) Parak, F.; Knapp, E. W.; Kucheida, D. *J. Mol. Biol.* **1982**, *161*, 177–194.
(6) Doster, W.; Cusack, S.; Petry, W. *Nature* **1989**, *337*, 754–756.
(7) Di Pace, A.; Cupane, A.; Leone, M.; Vitrano, E.; Cordone, L. *Biophys. J.* **1992**, *63*, 475–484.
(8) Hagen, J. S.; Hofrichter, J.; Eaton, W. A. *Science* **1995**, *269*, 959–962.
(9) Ringe, D.; Petsko, G. A. *Biophys. Chem.* **2003**, *105*, 667–680.
(10) Srajer, V.; Teng, T. Y.; Ursby, T.; Pradervand, C.; Ren, Z; Adachi, S.; Schildkamp, W.; Bourgeois, D.; Wulff, M.; Moffat, K. *Science* **1996**, *274*, 1726–1729.
(11) Bourgeois, D.; Vallone, B.; Schotte, F.; Arcovito, A.; Miele, A. E.; Sciara, G.; Wulff, M.; Anfinrud, P.; Brunori, M. *Proc. Natl. Acad. Sci. U.S.A.* **2003**, *100*, 8615–8617.
(12) Frauenfelder, H.; McMahon, B. H.; Fenimore, P. W. *Proc. Natl. Acad. Sci. U.S.A.* **2003**, *100*, 8704–8709.
(13) Brunori, M.; Bourgeois, D.; Vallone, B. *J. Struct. Biol.* **2004**, *147*, 223–234.
(14) He, Y.; Ku, P. I.; Knab, J. R.; Chen, J. Y.; Karkelz, A. G. *Phys. Rev. Lett.* **2008**, *101*, 178103–1−178103−4.
(15) Feher, V. A.; Cavanagh, J. *Nature* **1999**, *400*, 289–293.
(16) Song, X.-J.; Simplacenau, V.; Ho, N. T.; Ho, C. *Biochemistry* **2008**, *47*, 4907–4915.
(17) Bourgeois, D.; Royant, A. *Curr. Opin. Struct. Biol.* **2005**, *15*, 538–547.
(18) Bardy, K. L.; Setzer, D. R. *J. Biol. Chem.* **2005**, *280*, 16115–16124.
(19) Frauenfelder, H.; Fenimore, P. W.; Chen, G.; McMahon, B. H. *Proc. Natl. Acad. Sci. U.S.A.* **2006**, *103*, 15469–15472.
(20) Modig, K.; Liepinsh, E.; Otting, G.; Halle, B. *Proc. Natl. Acad. Sci. U.S.A.* **2004**, *126*, 102–114.
(21) Zhang, L.; Wang, L.; Kao, Y.-T.; Qiu, W.; Yang, Y.; Okobiah, O.; Ahong, D. *Proc. Natl. Acad. Sci. U.S.A.* **2007**, *104*, 18461–18466.

(22) Ackers, G. K.; Holt, J. M. *J. Biol. Chem.* **2006**, *281*, 11441–11443.
(23) Ma, B.; Elkayam, T.; Wolfson, H.; Nussinov, R. *Proc. Natl. Acad. Sci. U.S.A.* **2003**, *100*, 5772–5777.
(24) Massari, A. M.; Finkelstein, I. J.; McClain, B. L.; Goj, A.; Wen, X.; Bren, K. L.; Loring, R. F.; Fayer, M. D. *J. Am. Chem. Soc.* **2005**, *127*, 14279–14289.
(25) Gottfried, D. S.; Peterson, E. S.; Sheik, A. G.; Wang, J.; Yang, M.; Friedman, J. M. *J. Phys. Chem.* **1996**, *10z0*, 12034–12042.
(26) Frauenfelder, H.; Chen, G.; Berendzen, J.; Fenimore, P. W.; Jansson, H.; McMahon, B. H.; Stroe, I. R.; Swenson, J.; Young, R. D. *Proc. Natl. Acad. Sci. U.S.A.* **2009**, *106*, 5129–5134.
(27) Tsuneshige, A.; Yonetani, T. *Methods Enzymol.* **1994**, *231*, 215–222.
(28) Gonnelli, M.; Strambini, G. B. *Biochemistry* **1995**, *34*, 13847–13857.
(29) Vanderkooi, J. M.; Maniara, G.; Green, T. J.; Wilson, D. F. *J. Biol. Chem.* **1987**, *262*, 5476–5482.
(30) Tompa, P.; Bánki, P.; Bokor, M.; Kamasa, P.; Kovács, D.; Lasanda, G.; Tompa, K. *Biophys. J.* **2006**, *91*, 2243–2249.
(31) Tompa, P.; Bánki, P.; Bokor, M.; Kamasa, P.; Kovács, D.; Lasanda, G.; Tompa, K. *Biophys. J.* **2009**, *96*, 2789–2798.
(32) Fenimore, P. W.; Frauenfelder, H.; McMahon, B. H.; Young, R. D. *Proc. Natl. Acad. Sci. U.S.A.* **2004**, *101*, 14408–14413.
(33) Ansari, A.; Jones, C. M.; Henry, E. R.; Hofrichter, J.; Eaton, W. A. *Science* **1992**, *256*, 1796–1798.
(34) Fenimore, P. W.; Frauenfelder, H.; McMahon, B. H.; Parak, P. G. *Proc. Natl. Acad. Sci. U.S.A.* **2002**, *99*, 16047–16051.
(35) Schay, G.; Smeller, L.; Tsuneshige, A.; Yonetani, T.; Fidy, J. *J. Biol. Chem.* **2006**, *281*, 25972–25983.
(36) Karplus, M.; Ichiye, T.; Pettitt, B. M. *Biophys. J.* **1987**, *52*, 1083–1085.
(37) Carrero, J.; Jameson, D. M.; Gratton, E. *Biophys. Chem.* **1995**, *54*, 143–154.
(38) Tilton, R. F., Jr.; Kuntz, I. D., Jr.; Petsko, G. A. *Biochemistry* **1984**, *23*, 2849–2857.
(39) Cohen, J.; Arkhipov, A.; Braun, R.; Schulten, K. *Biophys. J.* **2006**, *91*, 1844–1857.
(40) Colombo, M. F.; Rau, D. C.; Parsegian, V. A. *Proc. Natl. Acad. Sci. U.S.A.* **1994**, *91*, 10517–10520.
(41) Miyazaki, G.; Morimoto, H.; Yun, K. M.; Park, S.-Y.; Nakagawa, A.; Minagawa, A.; Shibayama, N. *J. Mol. Biol.* **1999**, *292*, 1121–1136.
(42) Yonetani, T.; Laberge, M. *Biochim. Biophys. Acta* **2008**, *1784*, 1146–1158.
(43) Pin, S.; Royer, C.-A.; Gratton, E.; Alpert, A.; Weber, G. *Biochemistry* **1990**, *29*, 9194–9202.

■ NOTE ADDED AFTER ASAP PUBLICATION

This paper was published on the Web on March 11, 2011. Equations 7 and 8 were revised. The corrected version was reposted on March 21, 2011.